Electronic Supplementary Information

Synthesis, characterization, and reactivity of a chiral Fe(IV)-oxo complex bearing an L-proline derived aminopyridine ligand

Junyi Du,[ab] Jisheng Zhang,[a] Jianhua Zhu,[a] Chungu Xia[a] and Wei Sun*[a]

[a] *State Key Laboratory for Oxo Synthesis and Selective Oxidation, and Suzhou Research Institute of LICP, Lanzhou Institute of Chemical Physics (LICP), Chinese Academy of Sciences, Lanzhou, 730000, P. R. China*

[b] *University of Chinese Academy of Sciences, Beijing 100049, P. R. China*

* To whom correspondence should be addressed.

E-mail: wsun@licp.cas.cn

Table of Contents

General Remarks

All chemicals were purchased from commercial sources and used as received unless noted otherwise. Iodosylbenzene was prepared by a literature method.[S1] The ligand Pro3Py was synthesized following the reported procedures.[S2] Methyl 1-tetralone-2-carboxylate and racemic methyl 2-hydroxy-1-tetralone-2-carboxylate were synthesized according to literature methods.[S3, S4] The Fe^{II} complex was prepared according to the literature methods.[S5, S6] X-ray crystallographic data were collected on a Bruker SMART CCD1000 diffractometer with graphite-monochromated Mo Kα radiation (λ = 0.71073 Å). UV-vis spectra were recorded on an Agilent 8454 spectrophotometer equipped with a variable-temperature liquid-nitrogen cryostat (UNISOKU Scientific Instruments). CSI-TOF MS spectra were collected on a JMS-T100CS (JEOL) mass spectrometer equipped with a CSI source. Typical measurement conditions were as follows: needle voltage: 2.2 kV, orifice 1 current: 50-500 nA, orifice 1 voltage: 0 to 20 V, ring lens voltage: 10 V, ion source temperature: 5 °C, spray temperature: –40 °C. The CSI-TOF mass spectra of **2**-^{16}O and **2**-^{18}O were obtained by infusing the reaction solution directly into the ion source through pre-cooled tube under high N_2 gas pressure. EPR specturm was recorded on an X-band Bruker EMX-plus spectrometer equipped with a dual mode cavity (ER 4116DM). Low temperatures were achieved and controlled with Oxford Instruments ESR900 liquid Helium quartz cryostat fitted with an Oxford Instruments ITC503 temperature and gas flow controller. EPR conditions: temperature, 5 K; microwave frequency, 9.647 GHz; microwave power, 1.0 mW; modulation amplitude, 10 G; modulation frequency, 100 kHz. GC-MS analysis for products in the oxidation reactions of hydrocarbons were performed with Agilent 7890A/5975C GC-MS system with an HP-5 MS column. HPLC analysis for measuring enantiomeric excess (*ee*) values was performed with a SHIMADZU system (SHIMADZU LC-20AT pump, SHIMADZU LC-20A Absorbance Detector) with a Chiralpak OD-H column (Daicel Chemical Industries, LTD). The room temperature magnetic moment of 3.4 μ_B for **2** is recorded using the method of Evans,[S7] which is consistent with the low-spin (S = 1) Fe^{IV} center. Elemental analysis for **1** was conducted with a Vario EL cube Elemental analyzer. Anal. calcd for $C_{25}H_{27}F_6FeN_5O_6S_2$: C, 41.28; H, 3.74; N, 9.63; S, 8.81. Found: C, 41.40; H, 3.67; N, 9.59; S, 8.84.

References

(S1) H. Saltzman and J. G. Sharefkin, *Organic Syntheses*, 1963, **43**, 60-61.

(S2) J. Du, D. Xu, C. Zhang, C. Xia, Y. Wang and W. Sun, *Dalton Trans.*, 2016, **45**, 10131-10135.

(S3) L. Q. Cui, Z. L. Dong, K. Liu and C. Zhang, *Org. Lett.*, 2011, **13**, 6488-6491.

(S4) J. Yu, J. A. Cui and C. Zhang, *Eur. J. Org. Chem.*, 2010, **2010**, 7020-7026.

(S5) B. Wang, S. Wang, C. Xia and W. Sun, *Chem. Eur. J.*, 2012, **18**, 7332-7335.

(S6) M. Wu, C. X. Miao, S. F. Wang, X. X. Hu, C. G. Xia, F. E. Kühn and W. Sun, *Adv. Synth. Catal.*, 2011, **353**, 3014-3022.

(S7) D. F. Evans, *J. Chem. Soc.*, 1959, 2003-2005.

Table S1 Crystal Data and Structure Refinement for **1**-OTf

Empirical formula	$C_{25}\ H_{27}\ F_6\ Fe\ N_5\ O_6\ S_2$
Formula weight	727.49
Temperature (K)	296(2)
Wavelength (Å)	0.71073
Crystal system/space group	Orthorhombic/ $P2_12_12_1$
Unit cell dimensions	
a (Å)	9.0731(7)
b (Å)	14.0441(10)
c (Å)	24.1001(17)
α (º)	90.00
β (º)	90.00
γ (º)	90.00
Volume (Å^3)	3070.9(4)
Z	4
Calculated density (g cm^{-3})	1.573
Absorption coefficient (mm^{-1})	0.711
F(000)	1488
Reflections collected	15683
Independent reflections [R(int)]	5397 [0.0229]
Absorption correction	Multi-scan
Data/restraints/parameters	5085/0/406
Goodness-of-fit on F^2	1.007
Final *R* indices [*I*>2sigma(*I*)]	0.0400
Final *wR* indices [*I*>2sigma(*I*)]	0.1148
Largest difference peak and hole (e/Å^3)	0.512 and -0.352

Table S2 Selected Bond Distances (Å) and Angles (º) for **1**-OTf

Bond Distances (Å)	
Fe1-N1	2.175(3)
Fe1-N2	2.204(3)
Fe1-N3	2.168(3)
Fe1-N4	2.227(2)
Fe1-N5	2.216(3)
Fe1-O1	2.055(3)
Bond Angles (º)	
O1-Fe1-N1	95.1(1)
O1-Fe1-N2	160.1(1)
O1-Fe1-N3	87.3(1)
O1-Fe1-N4	114.8(1)
O1-Fe1-N5	91.2(1)
N1-Fe1-N2	75.4(1)
N1-Fe1-N3	100.5(1)
N1-Fe1-N4	146.0(1)
N1-Fe1-N5	89.5(1)
N2-Fe1-N3	77.5(1)
N2-Fe1-N4	80.2(1)
N2-Fe1-N5	106.0(1)
N3-Fe1-N4	96.8(1)
N3-Fe1-N5	170.0(1)
N4-Fe1-N5	74.8(1)

Table S3 C-H BDE Values of Substrates, Numbers of Equivalent Target C–H Bonds of Substrates (n), Second-Order Rate Constants (k_2), Apparent Second-Order Rate Constants (k_2') and log(k_2') Values, and Major Products in the C-H Bond Activation Reaction of Various Substrates by **2** in CH_3CN at 0 °C

entry	substrate	C-H BDE,[a] kcal mol^{-1}	k_2, M^{-1} s^{-1}	n	k_2',[b] M^{-1} s^{-1}	log(k_2')	major product
1	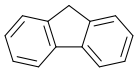	80.1	3.8	2	1.9	2.8×10^{-1}	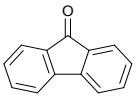
2		82.6	6.8×10^{-1}	4	1.7×10^{-1}	-7.7×10^{-1}	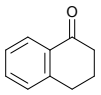
3		84.0	6.6×10^{-2}	1	6.6×10^{-2}	-1.2	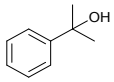
4		87.0	1.4×10^{-2}	2	7.0×10^{-3}	-2.2	
5	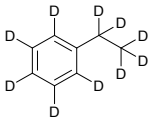	-	3.6×10^{-4}	-	-	-	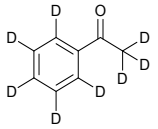

[a]Y.-R. Luo, *Comprehensive Handbook of Chemical Bond Energies,* CRC Press, Boca Raton, 2007.

[b]$k_2' = k_2/n$

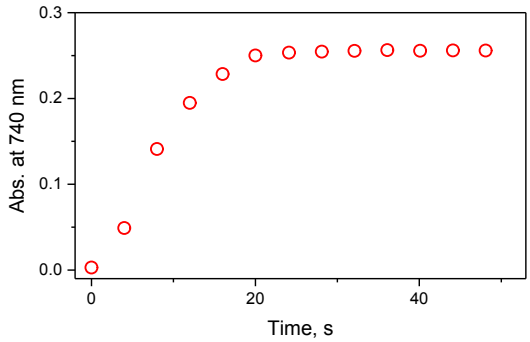

Fig. S1 Time course of UV-vis spectral changes monitored at 740 nm showing the formation of **2** in the reaction of **1** (1 mM) and PhIO (1.5 mM) in CH_3CN at 0 °C.

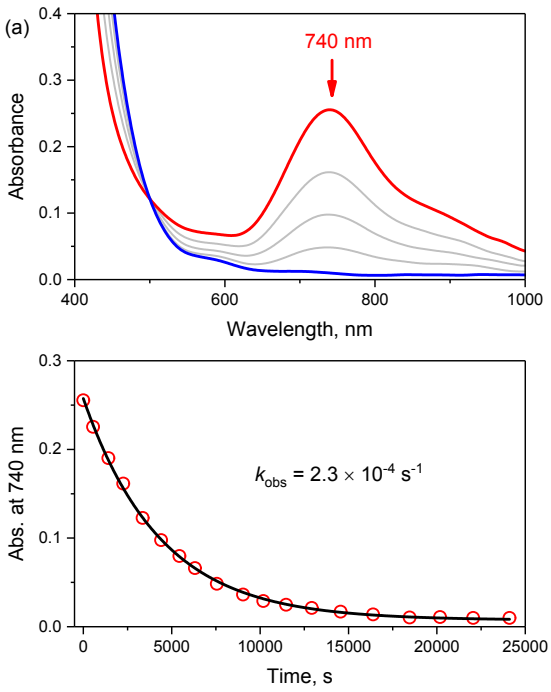

Fig. S2 (a) UV-vis spectral changes showing the natural decay of **2** (1 mM) in CH_3CN at 0 °C. (b) Time course monitored at 740 nm showing a pseudo-first-order natural decay profile.

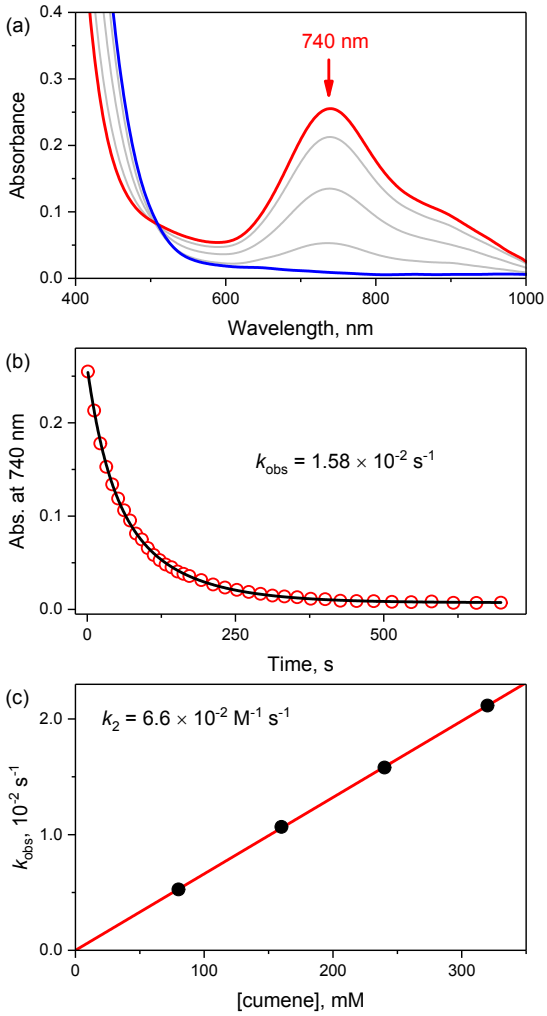

Fig. S3 (a) UV-vis spectral changes observed in the reaction of **2** (1 mM, red line) and cumene (240 mM) in CH_3CN at 0 °C (b) Exponential fitting (black curve) for the time trace (red circles) of **2** monitored at 740 nm in the reaction showing a pseudo-first-order decay profile. (c) Plot of the pseudo-first-order rate constant, $k_{obs}(s^{-1})$, against the concentration of cumene to determine the second-order rate constant, k_2 (M^{-1} s^{-1}) in the oxidation of cumene by **2** (1 mM) in CH_3CN at 0 °C.

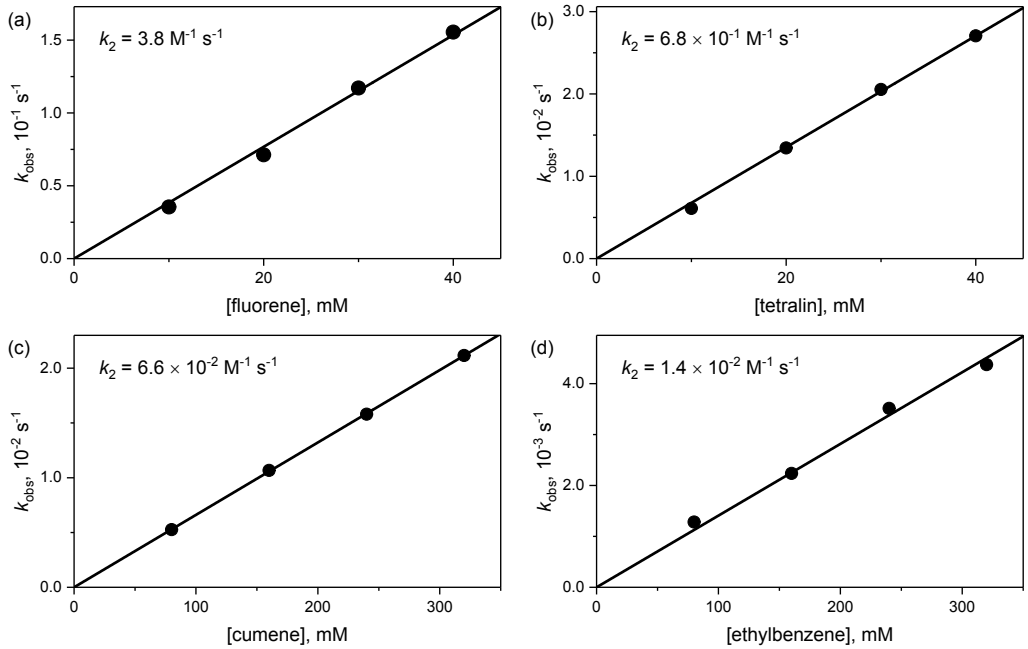

Fig. S4 Plots of pseudo-first-order rate constants (k_{obs}) against the concentrations of substrates [(a) fluorene, (b) tetralin, (c) cumene, (d) ethylbenzene] to calculate the second-order rate constant (k_2) in the C-H bond activation of hydrocarbons by **2** (1 mM) in CH_3CN at 0 °C (see also Table S3).

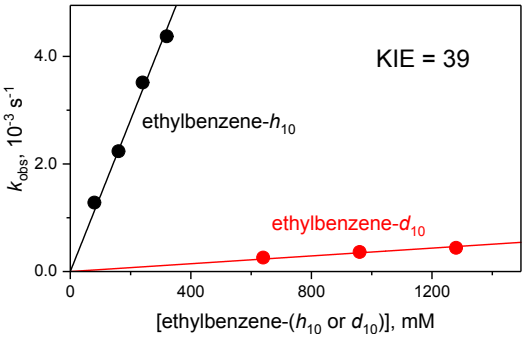

Fig. S5 Plots of k_{obs} against substrate concentration to calculate k_2 and KIE value in the reactions of **2** (1 mM) with ethylbenzene (black, k_2 = 1.3 × 10^{-2} M^{-1} s^{-1}) and ethylbenzene-d_{10} (red, k_2 = 1.7 × 10^{-4} M^{-1} s^{-1}) in CH_3CN at 0 °C (see also Table S3).

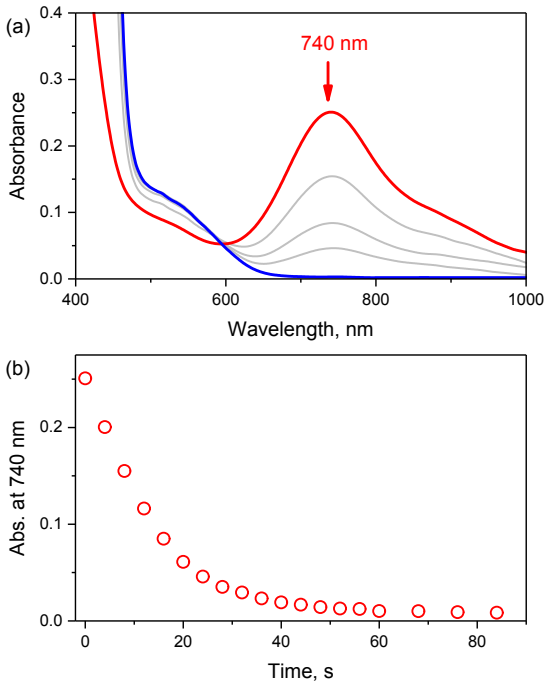

Fig. S6 (a) UV-vis spectral changes observed in the reaction of **2** (1 mM, red line) and thioanisole (7 mM) in CH_3CN at 0 °C. (b) The time trace of **2** monitored at 740 nm in the reaction.

Standard sample

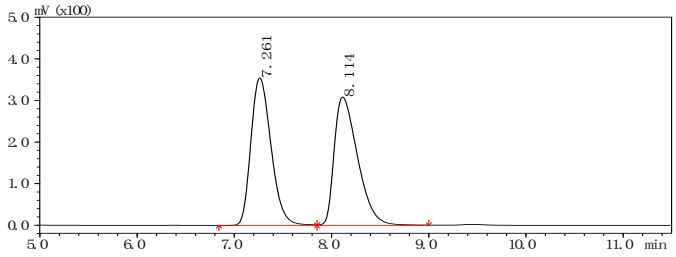

# Peak	Ret. Time	Area	Height	% Area
1	7.261	5109564	354235	49.738
2	8.114	5163414	308548	50.262

Reaction system

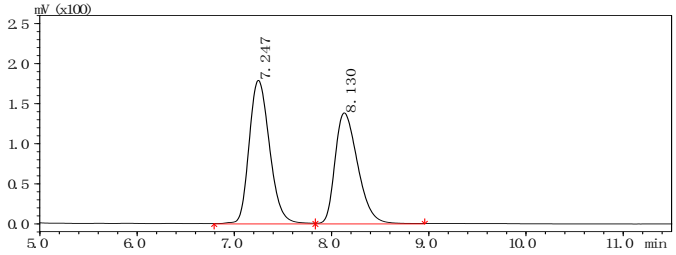

# Peak	Ret. Time	Area	Height	% Area
1	7.247	2635497	179221	53.803
2	8.130	2262886	138606	46.197

Fig. S7 HPLC chromatograms of thioanisole oxide (racemate) as an authentic compound (top) and the product (bottom) obtained in the oxidation of thioanisole (7 mM) by **2** (1 mM) in CH_3CN at 0 °C (*ee* 8%). HPLC separation condition: Chiralcel OD-H, 25 °C, 254 nm, 80/20 hexane/i-PrOH, 1 mL/min; t_{R1} = 7.2 min, t_{R2}= 8.1 min.

Standard sample

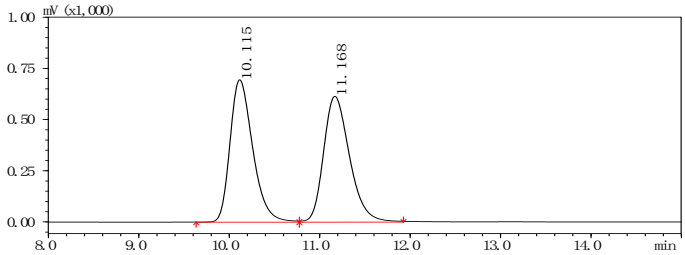

# Peak	Ret. Time	Area	Height	% Area
1	10.115	12171338	695951	49.768
2	11.168	12284607	614780	50.232

Reaction system

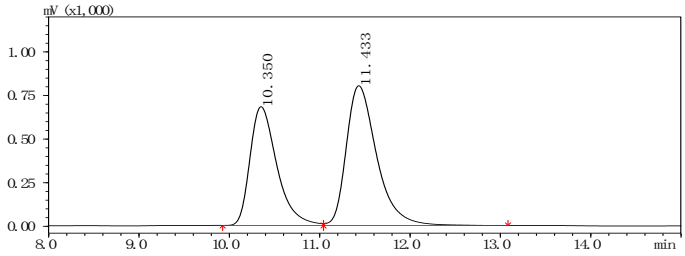

# Peak	Ret. Time	Area	Height	% Area
1	10.350	14123045	680824	42.908
2	11.433	18791913	801452	57.092

Fig. S8 HPLC chromatograms of methyl 2-hydroxy-1-tetralone-2-carboxylate (racemate) as an authentic compound (top) and the product (bottom) obtained in the oxidation of methyl 1-tetralone-2-carboxylate (20 mM) by **2** (1 mM) in CH_3CN at 0 °C under nitrogen atmosphere (*ee* 14%). HPLC separation condition: Chiralcel OD-H, 20 °C, 254 nm, 90/10 hexane/i-PrOH, 1 mL/min; t_{R1} = 10.1 min, t_{R2}= 11.2 min.

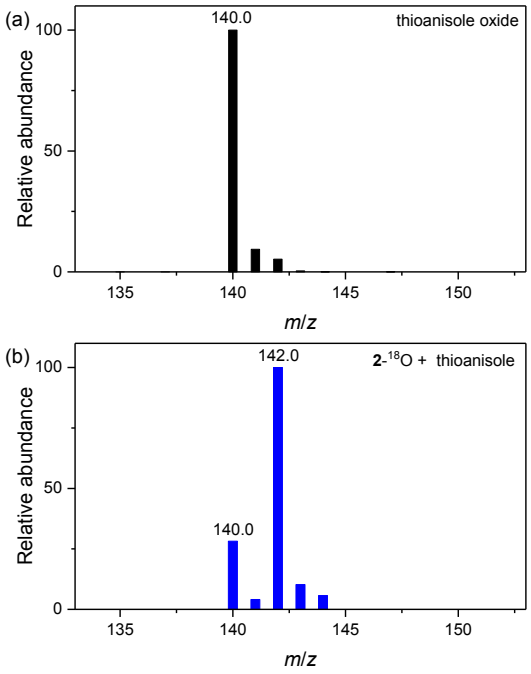

Fig. S9 GC-MS spectra of (a) thioanisole oxide-^{16}O as an authentic sample and (b) products obtained in the reaction of thioanisole (7 mM) with **2**-^{18}O (1 mM) in CH_3CN at 0 °C. The percentage of ^{18}O in the thioanisole product is 78%, which is determined by comparison of the relative abundances at m/z = 140 for thioanisole oxide-^{16}O and at m/z = 142 for thioanisole oxide-^{18}O.